Chapter 7 Appendix 1

CALCULATION OF THE BREN HOUSE SHIELDING EXPERIMENTS

William A. Woolson and Michael L. Gritzner
Science Applications International Corporation

Several American and Japanese institutions are engaged in research to produce and validate a revised dosimetry system for radiobiological analysis of the data about the survivors of the Hiroshima and Nagasaki A-bombs.[1-3] Correlative studies of the radiation dose with long-term health effects of these survivors are primary data on which modern radiation protection criteria are based.

The revised dosimetry system will be produced by modern calculational techniques, as distinguished from the dosimetry system presently used (called T65D), which relied mainly on nuclear weapons tests in Nevada and the Bare Reactor Experiment Nevada (BREN) experiments.[4] Data from materials exposed at Hiroshima and Nagasaki, the Nevada weapons tests, the BREN experiments, and other appropriate experimental data are being used to validate the techniques and computer codes used for calculations of the weapon-produced radiation sources, the air-over-ground radiation transport, the house shielding, and the in-body radiation transport.[1]

The calculation of the radiation emitted from the exploding bombs is described in Chapter 2; the calculation of the transport of initial radiation in air over ground, in Chapter 3; the calculation of the shielding by houses and terrain, in Chapter 7; the calculation of the self-shielding by the body, in Chapter 8.

As a first step in our research on the calculation of the shielding by houses, our methods were validated by comparing the results of our calculations with the results of the BREN house shielding experiments.[5] The BREN data were used to derive the "transmission factor" (see Chapter 7) used in T65D for Japanese houses. Although it was concluded that the experimental situation at BREN does not correctly represent the conditions in Hiroshima and Nagasaki,[6] the experimental data from BREN can still be used to validate our calculational procedures. Then these procedures can be used with models that represent more realistically the conditions in Hiroshima and Nagasaki to derive better house transmission factors (TF). This paper presents our work comparing calculated house TF with reported measured data from the BREN experiments.

Table 1. Distribution of Shielding Cases in Proximally Exposed Group

Category	Percentage		
	Combined	Hiroshima	Nagasaki
1. Open - Unshielded	7.3	8.1	5.6
2. Open - Partial Shielded	3.8	2.3	6.6
3. Open - Terrain	4.5	0.2	12.9
4. Open - Building Shielded	8.2	10.3	4.2
5. Concrete Building	3.5	1.6	7.2
6. Japanese House	51.8	58.3	39.3
7. Factory Building	4.3	0.2	12.5
8. Air-raid Shelter	1.4	0.2	3.9
9. Miscellaneous	0.3	0.2	0.4
Unknown	14.8	18.7	7.5
Total Cases	18770	12375	6395

Background

Detailed descriptions of the location and position at the time of bombing (ATB) of the A-bomb survivors in the Radiation Effects Research Foundation (RERF) data bases, such as the Life Span Study (LSS),[7] have been compiled from interviews and placed in shielding records. Nine categories were used in the computer files to describe the shielding situation of the survivor. The number of subjects in each category for the proximally exposed group (less than 1600 m ground range at Hiroshima and less than 2000 m at Nagasaki) is given in Table 1. Over half the survivors in the data base were inside residential houses ATB.

In the T65D system, the perturbation of the free-in-air (FIA, see Editor's Note) radiation by residential houses was given as TF for neutrons and gamma rays, which, when multiplied by the FIA kermas, gave the kermas inside the buildings.[4] Later, organ TF were developed to account for body self-shielding.[8] The house TF for individual survivors were calculated with a parametric model called the "Nine-Parameter Formula" (NPF) that was based on a regression analysis of the BREN house transmission experiments.[5] The nine parameters were derived from examination of the individual survivor's shielding records and were coded for computer access.[9]

The BREN house transmission experiments consisted of exposing radiation analogs of Japanese residential houses to radiation from the bare (unshielded) Health Physics Research Reactor (HPRR) and a ^{60}Co source.[5] The sources were mounted up to 1125 feet high in a tower, and the houses were placed at distances from 750 to 1200 yards from the base of the tower. The TF reported were the ratios of the neutron and gamma-ray kermas measured at various locations inside the houses to the kermas measured at the same ground ranges at locations free from local obstructions. The neutron measurements were made with a recoil-proton proportional counter, and the gamma-ray measurements were made with Geiger-Mueller tubes.

With this experimental procedure, the gamma-ray kerma measured inside the house includes gamma rays produced by neutron inelastic and capture reactions with the house materials. Thus, the gamma-ray TF are dependent on the local neutron field. For the nominal

configuration at BREN (HPRR at 1125 ft height, houses at 750 yd) the calculated neutron to gamma-ray kerma ratio is nearly three, while at Hiroshima and Nagasaki the same ratio is less than 0.1 and 0.01, respectively, at ground ranges where survivors in the data bases were present (beyond about 900 m). This difference was first examined by Marcum,[10] who concluded that the gamma-ray TF used in T65D and based on BREN data were too high by about a factor of 1.6.[6]

Although the BREN experiments did not accurately replicate the radiation fields at Hiroshima and Nagasaki, they were valuable experiments for validating calculational procedures that can then be applied to the Japanese house shielding problem. Our method for calculating the house shielding uses the Monte Carlo technique in the adjoint mode to compute the effect of the house cluster on the response function of a detector to radiations of different energies and directions. This response function can then be coupled to the FIA energy- and angle-differential fluences to estimate the response of the detector.

Theory

The radiation field inside a small structure far removed from a source of radiation can be determined by partitioning the problem into separate transport calculations that are then coupled to provide the overall solution. This partition consists of a calculation of the global radiation field in simplified geometry coupled to an appropriate radiation transport calculation in a detailed geometry model of the structure. The first calculation is a discrete ordinates numerical solution to the Boltzmann transport equation (BTE) in two-dimensional air-over-flat ground geometry; the latter calculation is often a Monte Carlo solution to the adjoint BTE in a three-dimensional model of the structure.

The theoretical basis for this solution technique is the fact that the radiation field inside a volume enclosed by a nonreentrant surface is completely determined by the incoming radiation fluence distributions in energy and direction and the radiation sources within the volume. Since the structures have no internal sources of radiation, the interior radiation field can be determined if the incoming particle fluences on a nonreentrant surface (e.g., a sphere or cylinder enclosing the structure) is known.

The theory for this procedure has been rigorously developed and adequately explained by many authors, notably Hoffman et al.[11] A summary is provided here only to maintain continuity for the reader. Following Hoffman et al, the rigorous solution to the complete problem (including both source and structure geometry) is given by

$$H\phi(\overline{P}) = S(\overline{P}) \tag{1}$$

where H is the Boltzmann operator, $\phi(\overline{P})$ is the flux in six-dimensional phase space (denoted by $\overline{P}$), and $S(\overline{P})$ is the source. The result of interest, λ (i.e., some observable quantity) involves integration of a known flux-response function, $R(\overline{P})$ with the particle flux,

$$\lambda = \int \phi(\overline{P}) R(\overline{P})\, d\overline{P} \tag{2}$$

Now, it is assumed that the source $S(\overline{P})$ is zero in the region of the structure and the response function $R(\overline{P})$ is zero outside the region of the structure. Let $\overline{r}_s$ denote the vector

of the locus of points describing a nonreentrant surface enclosing volume V containing the structure. Let $\overline{P}_V$ denote phase space elements in V. It is required that

$$S(\overline{P}_V) = 0 \tag{3}$$

and

$$R(\overline{P}) = 0, \quad \overline{P} \notin \overline{P}_V \tag{4}$$

In this case, the rigorous solution for the flux in V can be written as

$$H\phi(\overline{P}_V) = -(\overline{n}\cdot\overline{\Omega})\phi(\overline{P}_V)\delta(\overline{r}-\overline{r}_s)\,,\ \overline{n}\cdot\overline{\Omega} < 0 \tag{5}$$

where $\overline{n}$ is the outward directed normal to the nonreentrant surface, and the spatial and anglular elements of $\overline{P}$ are denoted by $\overline{r}$ and $\overline{\Omega}$, respectively. Equation 1 has been replaced for the flux in V by an equivalent expression with Equation 5.

The well-known property of the Boltzmann operator

$$\int_V \phi^*(\overline{P}_V)\,H\phi\,(\overline{P}_V)\,d\overline{P_V} = \int_V \phi(\overline{P}_V)\,H^*\phi^*\,(\overline{P}_V)\,d\overline{P_V} + \int_V (\overline{n}\cdot\overline{\Omega})\phi\,(\overline{P}_V)\,\phi^*(\overline{P}_V)\,\delta(\overline{r}-\overline{r}_s)\,d\overline{P_V} \tag{6}$$

reduces to

$$\lambda = \int_V \phi\,(\overline{P}_V)\,R(\overline{P}_V)d\overline{P_V} = -\int_V (\overline{n}\cdot\overline{\Omega})\phi(\overline{P}_V)\phi^*(\overline{P}_V)\delta(\overline{r}-\overline{r}_s)d\overline{P_V} \tag{7}$$

by noting that the left hand side of Equation 6 is zero since $H\phi(\overline{P}_V) = S(\overline{P}_V) \equiv 0$ and by substituting

$$H^*\phi^*(\overline{P}_V) = R(\overline{P}_V) \tag{8}$$

Here, H^* is the adjoint Boltzmann operator. By virtue of Equation 5, the result, λ, cannot depend on the outward directed flux on the surface of V. This suggests the boundary condition for the solution for $\phi^*(\overline{P}_V)$ as

$$(\overline{n}\cdot\overline{\Omega})\phi^*(\overline{P}_V)\delta(\overline{r}-\overline{r}_s) = 0\,,\ \overline{n}\cdot\overline{\Omega} \geq 0 \tag{9}$$

Thus, by solving Equation 8 for $\phi^*(\overline{P}_V)$ with the boundary condition given by Equation 9 (vacuum boundary), the result, λ, can be obtained via

$$\lambda = -\int (\overline{n}\cdot\overline{\Omega})\phi(\overline{P}_V)\phi^*(\overline{P}_V)\delta(\overline{r}-\overline{r}_s)d\overline{P_V}\,,\ \overline{n}\cdot\overline{\Omega} < 0 \tag{10}$$

from Equation 7.

Our solution, at this point, has no approximations. But the flux $\phi(\overline{P}_V)$ in Equation 10

contains the stucture in the problem. It is now solved for a new flux

$$H_a\phi_a(\overline{P}) = S(\overline{P}) \tag{11}$$

for the same source but in a simpler, approximate geometry without the details of the structure present, as embodied in the operator H_a. Then the following approximate result is formed

$$\lambda_a = -\int (\overline{n}\cdot\overline{\Omega})\phi_a(\overline{P}_V)\phi^*(\overline{P}_V)\delta(\overline{r}-\overline{r}_s)\,d\overline{P_V}\ ,\ \overline{n}\cdot\overline{\Omega} < 0 \tag{12}$$

with an error

$$\varepsilon = -\int (\overline{n}\cdot\overline{\Omega})\{\phi_a(\overline{P}_V) - \phi(\overline{P}_V)\}\phi^*(\overline{P}_V)\delta(\overline{r}-\overline{r}_s)d\overline{P_V}\ ,\ \overline{n}\cdot\overline{\Omega} < 0 \tag{13}$$

Note that $\phi^*(\overline{P}_V)$ is still the rigorous solution in $\overline{P}_V$.

To summarize, the effect of interest inside a complex structure in air-over-ground geometry was calculated by performing a surface integral of the adjoint flux computed in the complex geometry with the incoming surface flux from the source computed in a simplified geometry. The error of this approximate approach is directly associated with the difference in the incoming surface fluxes in the simplified geometry and the complex geometry. Thus, assuming 1) an accurate adjoint solution $\phi^*(\overline{P}_V)$ can be obtained, 2) the incoming flux on the surface surrounding the structure is not significantly perturbed by the presence of the structure, and 3) the calculation of the flux $\phi_a(\overline{P}_V)$ in the simplified geometry model is accurate, then the solution given by Equation 12 should be a reasonable estimate of the desired result in Equation 2.

Application of The Theory

A code system called VCS (Vehicle Code System)[12] was developed to calculate $\phi^*(\overline{P}_V)\delta(\overline{r}-\overline{r}_s)$ and perform the numerical integration of Equation 12 with the forward fluxes, $\phi_a(\overline{P}_V)$, from a calculation with the two-dimensional discrete ordinates code, DOT.[13] This code system was originally designed to calculate radiation protection factors for military vehicles such as tanks and armored personnel carriers. The VCS code has been adopted with some major and minor simplifications for the house shielding analyses. In the following, we discuss how our modified VCS code system is used to estimate the radiation fields in structures.

The calculation of the forward flux, $\phi_a(\overline{P}_V)$, is performed with the DOT code. The DOT code uses multigroup, multitable cross sections coupling neutron transport, gamma-ray production from inealstic and capture reactions, and gamma-ray transport. The method utilizes discrete ordinates in two-dimensional geometries (spherical, cylindrical, and slab). The cylindrical geometry is used for VCS calculations consisting of air over a flat ground plane with the source located above the ground on the axis of symmetry. This simplified two-material geometry is adequate for calculations of the BREN reactor and the ^{60}Co source suspended above the desert in Nevada. It was shown to be adequate for built-up areas such as Hiroshima and Nagasaki by comparing with models containing distant buildings.

The DOT code for cylindrical geometry provides a computer file of the energy and

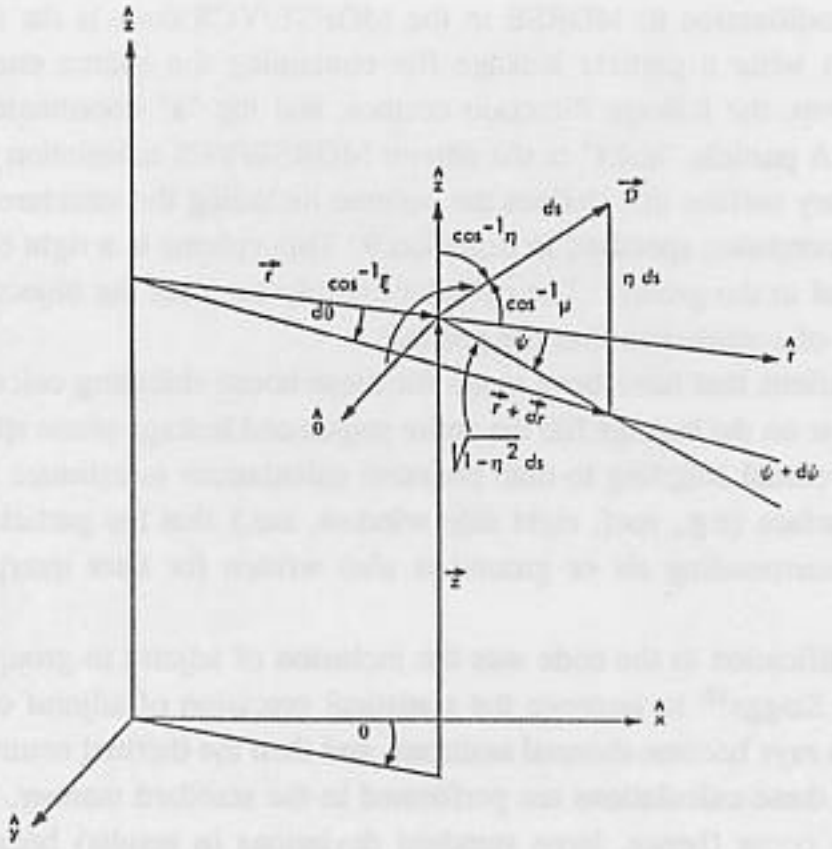

Figure 1. The coordinate system for cylindrical geometry

angular fluence distribution, $\phi_a(z, r, \eta, \psi, E)$, where the spatial coordinates (z, r) and angular coordinates (η, ψ) are defined in Figure 1. Note that η refers to the cosine of the angle of the direction with the z axis and ψ is the angle of the projection in the x-y plane with respect to the radial vector. (The subscript "a" for approximate is retained to note that the calculation does not include the specific structure in which the radiation field is desired.) The fluence is provided for discrete mesh intervals in z, r space, in η, ψ angular space, and for energy groups in E. Let ω_{ij} be the fraction of 4π angular space ascribed to the discrete ordinate (η_i, ψ_{ij}). The scalar fluence can be calculated as

$$\phi_a(z, r, E) = \sum_i \sum_j \phi_a(z, r, \eta_i, \psi_{ij}, E)\, \omega_{ij} \tag{14}$$

The angular fluence from DOT is the number of particles per cm^2 per fraction of 4π space. The VISA code of VCS is used to access the DOT angular flux file and retrieve only flux values near the air/ground interface required for the coupling calculation of Equation 12.

The adjoint quantity, $\phi^*(\overline{P}_V)\delta(\overline{r} - \overline{r}_s)$, is computed with an adaptation of the MORSE Monte Carlo code[14] called MORSE/VCS. The MORSE code uses multigroup, multitable cross sections and operates in both the forward and adjoint mode. Special user routines can be written and interfaced with MORSE to handle source specifications and flux estimation. Transport calculations can be carried out in complex geometrical configurations modeled with the combinatorial geometry package in MORSE.

The primary modification to MORSE in the MORSE/VCS code is the inclusion in the code of routines to write a particle leakage file containing the source energy group, the leakage energy group, the leakage direction cosines, and the "z" coordinate (height above the ground plane). A particle "leaks" in the adjoint MORSE/VCS calculation when it crosses the vacuum boundary surface that defines the volume including the structure, in accordance with the boundary condition specified in Equation 9. This volume is a right circular cylinder with the axis normal to the ground. The cylinder entirely encloses the object of interest and extends a few tens of centimeters into the ground.

Minor modifications that have been made for these house shielding calculations include the provision to write on the leakage file the entire source and leakage phase space parameters. This will enable eventual coupling to man phantom calculations to estimate body shielding. The geometrical surface (e.g., roof, right side window, etc.) that the particle crossed when escaping into the surrounding air or ground is also written for later interpretation of the results.

The major modification to the code was the inclusion of adjoint in-group biasing developed by Scott and Staggs[15] to improve the statistical precision of adjoint coupled calculations where gamma rays become thermal neutrons, and then the thermal neutrons upscatter to higher energies. If these calculations are performed in the standard manner, large variations in particle weights occur (hence, large standard deviations in results) because the adjoint thermal neutrons are "forced" to upscatter with a large fair game weight correction.

The adjoint calculation is performed with a detailed mathematical model of the structure using the combinatorial geometry package available with MORSE. The model contains the ground and air surrounding the structure inside the leakage surfaces of the cylinder. The adjoint simulation commences at the detector location in the structure. As the adjoint particle interacts with the materials in the building, air, and/or ground, it gains energy, and gamma rays produce adjoint secondary neutrons. The selection of scattered energy and angle uses the same procedures and routines as the forward calculation procedure, except the reaction cross sections for adjoint calculations are inverted from the forward set. When a particle leaks from the system, the relevant parameters are written to the leakage file and a new history is started.

When the calculation is completed, this leakage file contains the individual statistical weights of all the leaking particles as a function of source and leakage variables. The weight may be written as $W(\overline{R}_L, \overline{\Omega}_L, E_L, \overline{R}_s, \overline{\Omega}_s, E_s)$, where W is the statistical weight of the particle, and $(\overline{R}_L, \overline{\Omega}_L, E_L)$ and $(\overline{R}_s, \overline{\Omega}_s, E_s)$ are the leakage and source position, angle, and energy phase space parameters, respectively. The following notation

$$R_L = (x_L, y_L, z_L) \tag{15}$$

was employed to decompose the spatial vector into individual orthogonal components.

The DRC code of VCS reads the DOT forward flux tape prepared by VISA and the adjoint leakage file provided by MORSE/VCS and then performs the numerical integration of Equation 12.

Because the structure, in principal, can be oriented in any direction with respect to the source, the angular coordinates of each leakage particle are transformed to the desired

orientation. This transformation with a matrix derived from Eulerian angle rotation is given by

$$\overline{\Omega}'_L = \overline{\overline{T}} \cdot \overline{\Omega}_L \tag{16}$$

$$\overline{\Omega}'_s = \overline{\overline{T}} \cdot \overline{\Omega}_s \tag{17}$$

where $\overline{\overline{T}}$ is the transformation matrix. The standard VCS code permits only rotation of the structure about an axis parallel to the z direction. The generalized rotation has been added to examine the effects of small "tilts" in the structure, even though the ground planes of the DOT and adjoint calculations would not precisely align.

With the transformed angle coordinates, the angular bin of the DOT quadrature containing the leakage direction is found. First, the "eta" level is determined based on the value

$$\eta = \hat{z} \cdot \overline{\Omega}'_L \tag{18}$$

where $\hat{z}$ is the unit vector normal to the ground plane. The relative weight (or fraction of 4π space) associated with each polar eta level is calculated by DRC via

$$\omega_i = \sum_j \omega_{ij} \tag{19}$$

and the "i" index (eta level) is found such that

$$\sum_{i'=1}^{i-1} \omega_i \,, \leq \frac{1}{2}(\eta + 1) < \sum_{i'=1}^{i} \omega_i \,, \tag{20}$$

The phi level ("j" index) is based on the value:

$$\cos\psi_i = \hat{r} \cdot \overline{\Omega}'_L \sqrt{1 - \eta_i^2} \tag{21}$$

where $\hat{r}$ is the unit vector in the radial direction and is found via

$$\frac{1}{\omega_i} \sum_{j'=1}^{j-1} \omega_{ij} \,, \leq \frac{1}{2}(\cos\psi_j + 1) < \frac{1}{\omega_i} \sum_{j'=1}^{j} \omega_{ij} \,, \tag{22}$$

This procedure determines the discrete ordinate $\Omega_{ij} = (\eta_i, \psi_{ij})$ for the DOT angular flux.

The estimate of the fluence by Equation 12 is then given by

$$\phi(r_s, \overline{\Omega}'_s, E_s) =< \phi_a(z_L, r_s, \Omega_{ij}, E_L) \cdot W(\overline{R}_L, \overline{\Omega}'_L, E_L, \overline{R}_s, \overline{\Omega}'_s, E_s) > \tag{23}$$

where r_s is the ground range of the in-structure detector from the source in the DOT calculation, and the brackets < > indicate the average over the leakage variables for all histories. Note that this estimate depends only on the "z" spatial coordinate of the adjoint leakage.

The forward DOT flux for the coupling is only defined at the radius of the detector location r_s. This assumes that the variation in flux with radius is small compared to the radial extent of the structure.

By preserving the full phase space parameters of the adjoint source, the full energy-angular distribution of the fluence at the detector can be calculated. This can be used for detailed calculations of radiation transport in a phantom using the same surface integral technique (Equation 12) with an additional adjoint calculation in the phantom starting at the organ location. This facility to "nest" calculations using successive adjoint calculations was incorporated by us into the standard version of VCS. This was done by defining the angular fluence in the same angle bins as the DOT quadrature, so that the fluence calculated from a coupling procedure is in the same format as the VISA-processed DOT angular flux.

The fluence inside the structure can be used to calculate detector responses and kermas via

$$\lambda(r_s) = \int \phi(r_s, \overline{\Omega}'_s, E_s) R(E_s) d\overline{\Omega}'_s dE_s \tag{24}$$

where $R(E_s)$ is the energy-dependent response. Note that if the energy- and angular-dependent response is known, it can be integrated with the angular dependence of the fluence inside the building.

In addition to the approximation introduced by the theory, the practical application with the VCS methodology introduces approximations and sources of uncertainty. There exist the usual sources of uncertainty associated with any calculational technique: the knowledge of the physical variables associated with the configuration (e.g., air density, construction materials, structure layout), the basic data input to the calculation (e.g., nuclear cross sections), and modeling of the configuration and the physics data (e.g., number of geometry regions, energy group structures, quadrature order).

There are also sources of uncertainty peculiar to the surface integral coupling method. One of the most important is the coupling to DOT fluences at a single radial point corresponding to the ground range of the detector. Although VCS performs the surface integral as a function of a z coordinate, the code assumes the fluence does not vary in the radial direction across the leakage surface. To analyze this assumption, the radial variation of the fluence was written approximately as

$$\phi(r) \propto \frac{e^{-r/L}}{r^2} \tag{25}$$

for some appropriate relaxation length, L. This is a good representation over a limited range at least and was used, for example, in the T65D system to provide the doses at all ground ranges used by RERF. For small Δr, it can be written

$$\frac{\phi(r) - \phi(r + \Delta r)}{\phi(r)} \sim \Delta r \left[\frac{1}{L} + \frac{2}{r} \right] \tag{26}$$

The relaxation length is on the order of 300 m for many sources in air-over-ground, and, choosing r to be the same, it was estimated as a near worst case (since r is usually larger),

that the fluence changes by 10% in 10 m. This indicates that the assumption is reasonable for most structures.

Another issue that is more difficult to analyze is the adequacy of the resolution of the angular fluence in the DOT quadrature. The VCS procedure assumes the fluence is constant within the solid angle defined by the quadrature boundaries. Furthermore, the uncollided particles are "smeared" over the most forward directed quadrature interval. The concern is that streaming paths, such as windows, may receive too many or too few incident particles, depending on their relation to the quadrature boundaries and the "true" angular variation of the fluence.

Comparison with BREN Experiments

BREN House Transmission Measurements. Operation BREN experiments took place at the Nevada Test Site (NTS) in the spring of 1962.[16] The experiments consisted of supporting a small unshielded reactor and a ^{60}Co source in a tower at heights of up to 1125 feet and making measurements of free-field and house-perturbed neutron and gamma-ray kermas. The ratios of the kermas measured at detectors in (and around) the houses to the free-field kermas were reported as the house TF for the detector locations.

The HPRR was used for the neutron (and secondary gamma-ray) source.[17] The reactor consisted of a highly enriched uranium-molybdenum alloy metal annulus with an outside diameter of 0.203 m and inside diameter of 0.05 m. Details of the reactor configuration are found in Reference 17. The small size of the reactor and the lack of a reflector provided a hard, nearly unmoderated fission spectrum of neutrons. The ^{60}Co source used at BREN contained 1200 Ci at the time of manufacture, which had decayed to 800 Ci at the time of the experiments.

The free-field gamma-ray kermas produced by the HPRR and the ^{60}Co source were measured with the "Phil" detector described by Wagner and Hurst.[18] It consisted of a small Geiger-Mueller tube that was enclosed by tin and lead sheaths to provide a more uniform kerma per count as a function of the incident gamma-ray energy. When a neutron field was present, the Phil was further enclosed by a ^{6}Li shield to reduce the neutron response from thermal neutron capture. It was claimed that the Phil had negligible fast neutron response. To improve counting statistics during the ^{60}Co source runs, measurements inside the houses were performed with a larger Geiger-Mueller detector. The neutron kerma measurements were made with the RADSAN proportional counter.[19]

The houses constructed at NTS for the BREN experiments were designed to be radiation analogs of typical Japanese residential houses at Hiroshima and Nagasaki ATB.[5] Three models were built, designated as House A (a typical one-story family house), House B (a larger two-story residence), and House C (a small one-story tenement house). The houses were constructed full scale to the very uniform dimensions of Japanese dwellings. In place of Japanese construction materials, however, the designers used a cement asbestos board produced by the Johns Manville Corporation under the trade name TRANSITE, which was used in many houses in East Tenessee near the Oak Ridge National Laboratory (ORNL).[20] The use of the cement asbestos board was justified by the results of direct beam radiation measurements at ORNL that showed the ratio of PuBe neutron attenuation to ^{60}Co attenuation was similar to the ratio for a Japanese house wall section.[20,21] The exterior walls consisted

of 1-inch and 3/4-inch thick sheets butted together and placed in slots on wood-framing members. The interior walls were actually thicker and consisted of two 1-inch sheets. The roof had the same total thickness as the exterior walls but was composed of two 1/2-inch sheets and a 3/4-inch sheet.

The house models were built on skids enabling them to be towed and placed into different configurations and orientations. In addition, single walls of some of the houses were built and could be moved from place to place to produce additional shielding effects.

Free-in-air Environment. The VCS code system is designed to couple the adjoint calculation of building response with FIA fields calculated with the discrete ordinates code DOT. Calculations with DOT of the free-field radiation fields produced by the BREN ^{60}Co and BREN HPRR reactor used in the study were performed by Dolatshahi and Kaul.[22] A summary of the comparison of their calculations is provided here with the measurements of the FIA kerma made during the BREN experiments. A comparison of the kerma computed by DOT with measurements for the BREN ^{60}Co source at a height of 1125 feet is presented in Figure 2. The "r^2 kerma" as a function of slant range is presented at the air/ground interface.

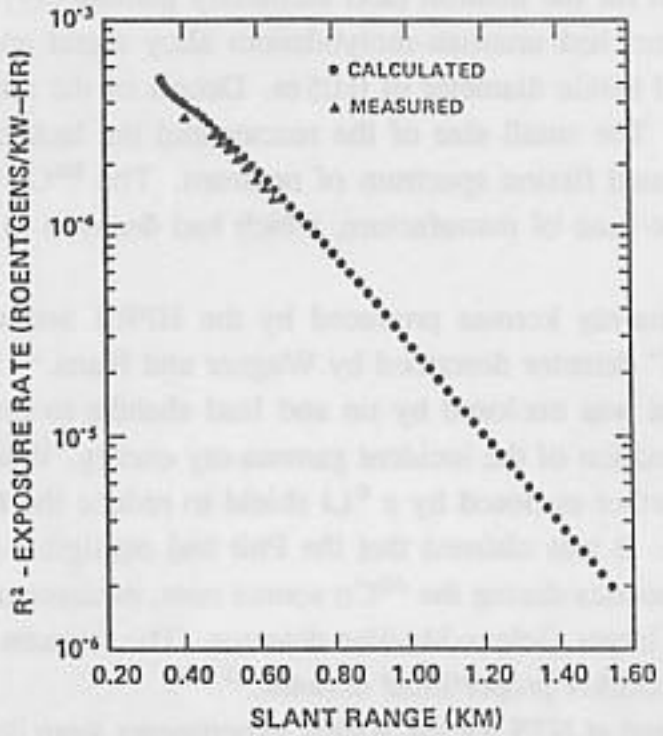

Figure 2. BREN ^{60}Co exposure rate versus slant range measured and calculated at the ground surface

This comparison and comparisons at other detector heights[22] show excellent agreement between the FIA calculations and the measurements. Similar comparisons of the neutron kerma from the HPRR reactor are presented in Figure 3. The DOT calculations for the neutron kerma are in excellent agreement with measurements at all heights for all ground ranges. However, calculated gamma-ray kermas associated with the HPRR source do not agree well with experiment, as indicated in Figure 4, with the calculations consistently low by about

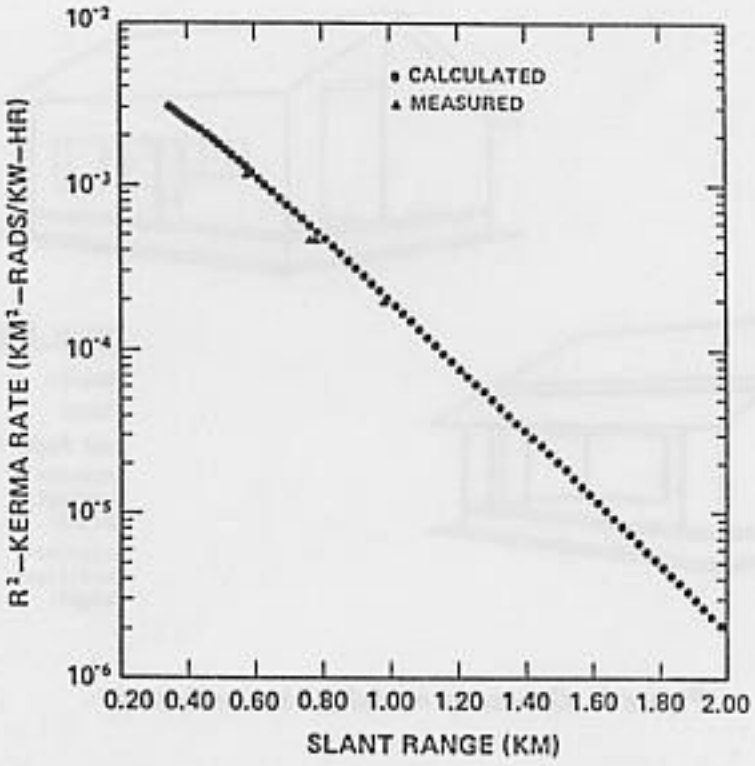

Figure 3. BREN reactor neutron kerma rate versus slant range measured and calculated at the ground surface

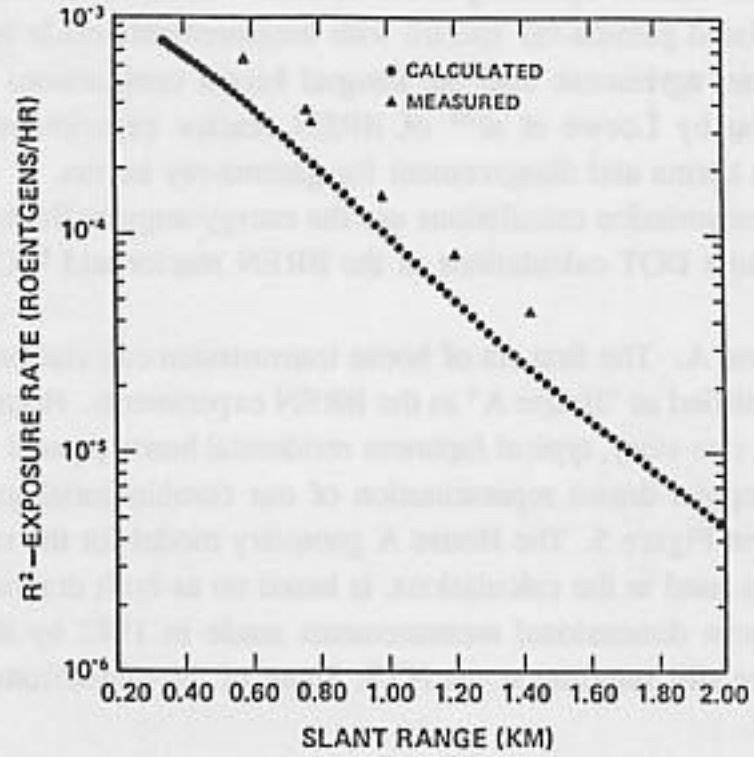

Figure 4. BREN reactor gamma-ray kerma rate versus slant range measured and calculated at the ground surface

40%. As discussed in Reference 22, the cause of this discrepancy is unresolved. Dolatshahi and Kaul have examined the calibration of the gamma-ray detector for the high energy gamma rays from the neutron-induced capture gamma rays, the neutron interactions with

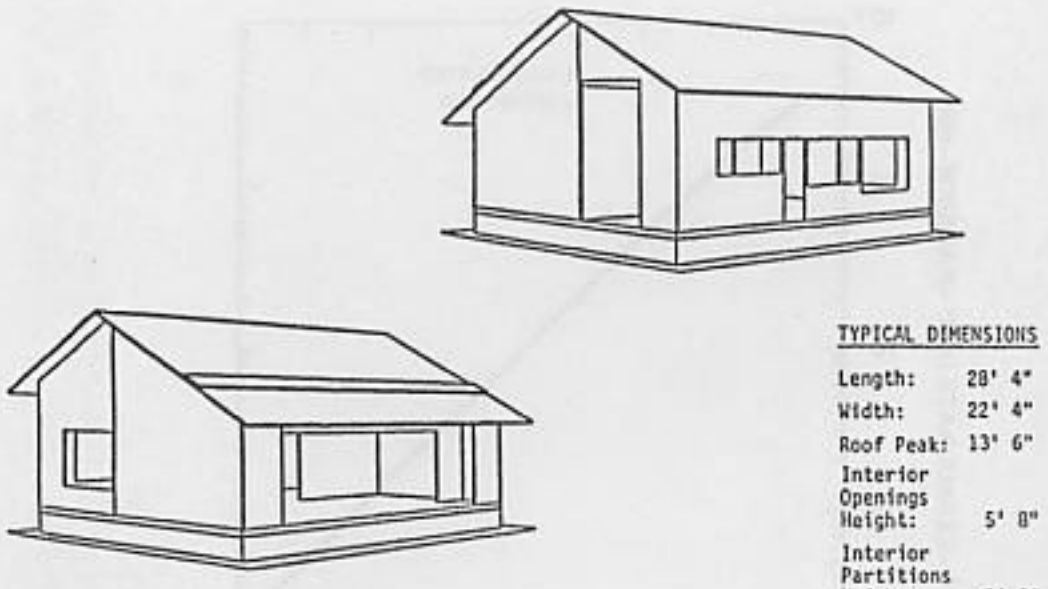

Figure 5. Geometry model for house Type A

the detector system that generate gamma rays, and the possibility that the neutron shield consisted of depleted or natural Li in place of ^{6}Li.[22] The same calculational technique has been applied to a similar reactor operating at the Ballistic Research Laboratory in Maryland. Comparisons of calculated gamma-ray spectra with measurements made with a NE-213 detector show much better agreement than the integral kerma comparisons for BREN.[22] An independent calculation by Loewe et al[23] of BREN reactor experiments exhibits similar agreement for neutron kerma and disagreement for gamma-ray kerma.

All of our house transmission calculations use the energy-angular fluence tapes produced by Dolatshahi and Kaul's DOT calculations of the BREN reactor and ^{60}Co experiments.

Calculations for House A. The first set of house transmission calculations were performed for a house model identified as "House A" in the BREN experiments. House A was designed to replicate a standard, one-story, typical Japanese residential house present at both Hiroshima and Nagasaki. A computer-drawn representation of our combinatorial geometry model of House A is presented in Figure 5. The House A geometry model for the radiation transport, as well as other houses used in the calculations, is based on as-built drawings obtained from NTS personnel and from dimensional measurements made in 1982 by the authors on the house frames that were still standing at the NTS. Some of the dimensions for House A are indicated in the figure.

Samples of the cement asbestos board used for the house walls, partitions, and roofs were obtained from the NTS in the vicinity of the houses, and an elemental analysis was performed at the ORNL.[24] The result of this analysis is presented in Table 2. Calculations for the ^{60}Co source used the "PVC" cross-section set[25] consisting of P_5 Legendre expansion of the scattering angular distributions and 36 energy groups for gamma-ray transport. Calculations for the HPRR source used the DLC-31 P_3 expanded cross sections in coupled multigroups (37 neutron groups - 21 gamma-ray groups).[26] Elemental cross sections available in both libraries

Table 2. Composition of Dry TRANSITE Sample[a]

Element	Concentration[b]	Available Cross Sections[c]	Element	Concentration[b]	Available Cross Sections[c]
H	1.43%	X	Zn	32.7	
Li	14.2	X	Ga	3.4	
Be	0.44	X	As	4.3	
B	11.8	X	Br	1.0	
C	3.73%	X	Rb	7.1	
N	0.011%	X	Sr	260.0	
O	50.9%	X	Y	3.88	
Na	774.0	X	Zr	21.7	
Mg	13.7%	X	Nb	5.2	
Al	1.06%	X	Mo	0.42	X
Si	12.8%	X	Ag	0.20	
Cl	169.0	X	Sb	0.18	
P	170.0	X	Ba	53.8	X
K	0.201%	X	La	5.3	
Ca	13.7%	X	Ce	11.1	
Sc	4.6		Sm	0.9	
Ti	542.0	X	Eu	0.28	
V	30.2	X	Tb	0.32	
Cr	650.0	X	Hf	0.93	
Mn	581.0	X	Ta	0.22	X
Fe	2.94%	X	W	0.20	X
Co	44.2		Pb	3.3	X
Ni	761.0	X	Th	1.8	X
Cu	5.05	X	U	0.69	X
			Total	100.9%	

[a]Dried 24 hours at 105 to 110°C with 1.08% moisture loss.

[b]Concentration in ppm by mass, except where noted as mass percent.

[c]Used PVC and DLC-31 Cross Section Libraries.[24,25] Elements mixed at reported concentration for dry TRANSITE. Those elements without corss sections are 0.04% by mass of the composition.

(indicated in Table 2) were mixed at the measured concentrations to form the macroscopic cross section for dry TRANSITE. Those elements without cross sections compose 0.04% of the mass of the composition. Our calculations employed a partial density of 2.08 g/cm^3 for TRANSITE plus a partial density of 0.023 g/cm^3 of mositure. Simple geometry ^{60}Co attenuation measurements of the house material were made at our laboratory by Shreve.[27] A comparison of the attenuation measurements, with the attenuation predicted by the cross sections used in our calculations, is shown in Figure 6.

Calculations using VCS were performed for House A for several different locations and detector heights. Our calculations for House A and other configurations were not designed to be exhaustive, but a representative comparison with the variety of measurements. The detector positions selected for calculation exhibit a variety of shielding situations: close to outside window or wall, near interior partition, and in room center. Furthermore, our results have not been edited; every calculation that was performed to compare with BREN experiments is presented. The detector locations are indicated in Figure 7, which presents a computer drawing of our House A model looking down from the top with no roof, showing the interior partitions and openings. The detector identification system is identical to the one used to report the BREN measurements.[5] The house was oriented so that the large opening

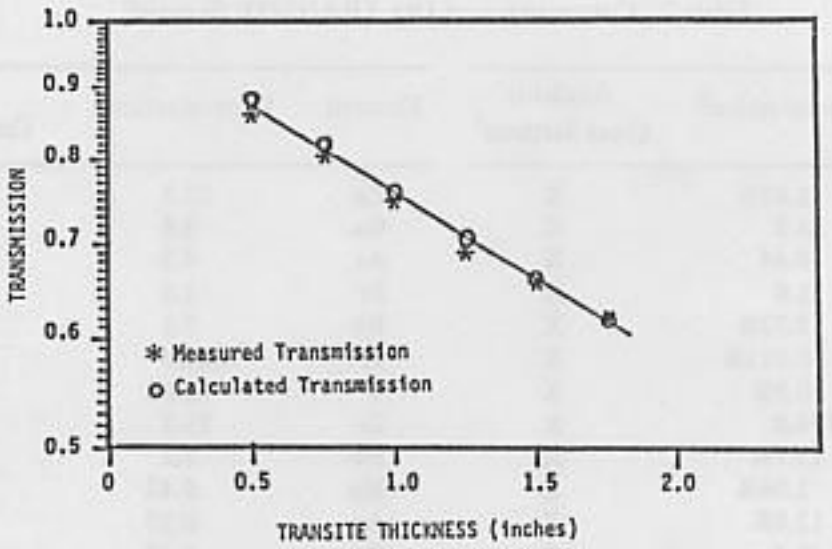

Figure 6. ^{60}Co (1.332 MeV γ) transmission in TRANSITE material

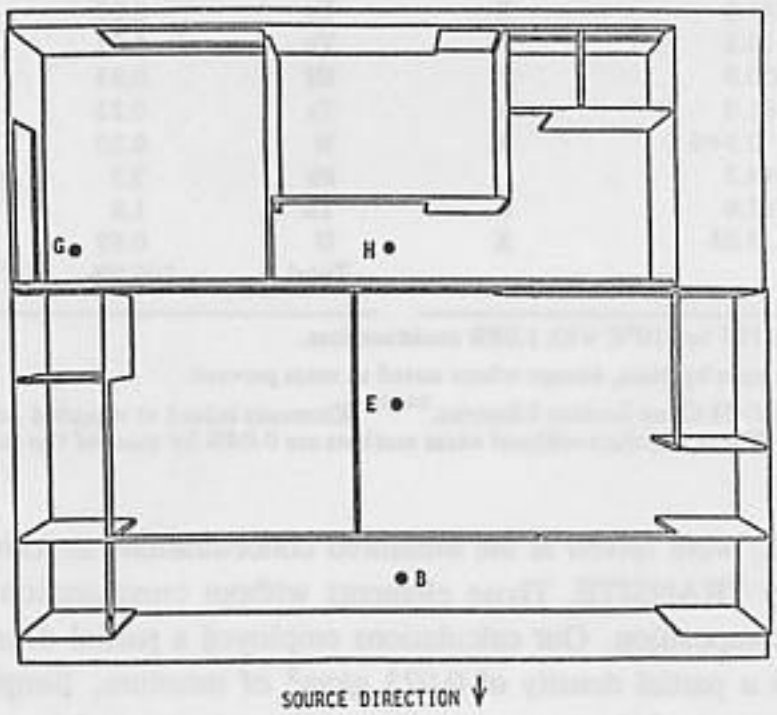

Figure 7. Interior of House A showing location of detectors

(the veranda) faced the source. The source was located at a ground range of 750 yards and a height of 1125 feet. Comparison of the calculated and measured TF for House A for the ^{60}Co source and the HPRR source are presented in Table 3. For both the measured and the calculated values, the TF is the in-house kerma divided by the corresponding free-field kerma. The HPRR gamma rays include prompt gamma rays emitted from the reactor, secondary gamma rays produced in the air and ground, and secondary gamma rays produced in the house materials. The comparison between the measured and calculated data for the ^{60}Co gamma-ray source is excellent. The neutron TF are also in excellent agreement with the measured data. Since part of the calculational procedure involves the numerical calculation

Table 3. Comparison of Calculations with Measurements of Transmission Factors for House A

Detector		^{60}Co Gamma rays		HPRR Neutron		HPRR Gamma rays	
Location	Height	Measured	Calculated	Measured	Calculated	Measured	Calculated
B	3 ft	0.62	0.63	-	-	-	-
E	3	0.56	0.55	0.48	0.48	-	-
E	5	0.40	0.41	0.46	0.44	1.44	1.02
G	5	-	-	0.48	0.44	-	-
H	3	0.40	0.44	0.41	0.43	1.32	0.97
H	5	-	-	0.43	0.38	-	-

Table 4. Gamma-ray Transmission Analysis for House A and HPRR Source

Component	FIA Kerma	Location H 3 ft		Location E 5 ft	
		Gamma-ray TF	Gamma-ray Kerma	Gamma-ray TF	Gamma-ray Kerma
Air/Ground Secondaries	0.744[a]	0.323	0.240	0.362	0.269
Prompt	0.256	0.441	0.113	0.488	0.125
Total Gamma rays	1.00	0.353	0.353	0.394	0.394
Neutron	2.90	0.214[b]	0.621	0.215[b]	0.624
		Total Calculated	0.97		1.02
		Measured	1.32		1.44

[a]All values normalized to the calculated free-in-air (FIA) total gamma-ray kerma

[b]Multiplys neutron FIA kerma to give gamma-ray kerma fraction (e.g., 0.621 at location H, 3ft) from secondary gamma-ray production in house materials

of the FIA field, it is not possible to provide a computed estimate of the statistical uncertainty in the calculated results. However, the fractional standard deviations involved in the adjoint Monte Carlo calculations are all less than 5%.

The comparison of the calculated gamma-ray TF from the HPRR source with the measured values, however, is not very good. At the two interior locations attempted, the calculated values are consistently lower than the measured data. The contributions to the gamma-ray TF calculated are provided in Table 4. All values in the table are normalized to the FIA total calculated gamma-ray kerma. At the location of the house (750 yd ground range), approximately 75% of the FIA kerma comes from secondary gamma rays produced by the neutrons in the air and in the ground, and the other 25% is from the prompt gamma rays emitted from the reactor. The neutron kerma at this point is almost three times higher than the gamma-ray kerma. At the 5-foot detector height for location E, our calculation of the gamma-ray kerma is nearly identical to the FIA gamma-ray kerma. In this instance, the gamma rays produced from neutron capture in the TRANSITE material offset the attenuation of the incident gamma-ray kerma. A similar situation exists for the 3-foot location H detector.

Since the gamma-ray TF for the prompt gamma rays and air secondary gamma rays ap-

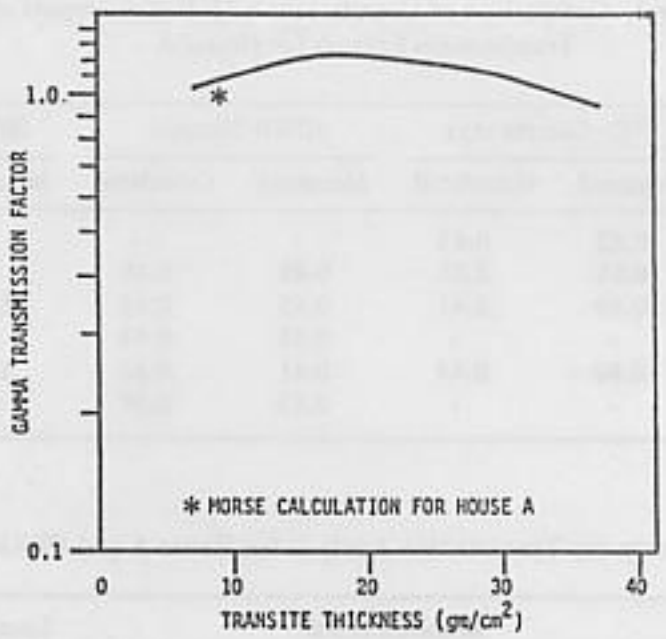

Figure 8. Maximum transmission factor model calculation for TRANSITE material

pear reasonable, it was conjectured that the discrepancy between the calculated and measured values stems from the production of gamma rays in the house materials. To test this supposition, a one-dimensional spherical discrete ordinates calculation with the ANISN code[28] was performed for a shell source of the BREN HPRR neutron and gamma-ray spectrum at 750 yards ground range incident on spherical shells of varying TRANSITE thickness. The calculated gamma-ray TF at the center of the sphere is given in Figure 8. The gamma-ray TF is the ratio of the gamma-ray kerma at the center of the sphere to the gamma-ray kerma at the shell source position. As the TRANSITE increases in thickness, the gamma-ray TF increases because of the increased production of capture gamma rays. However, beyond a certain thickness, the self-shielding of these capture gamma rays in the TRANSITE reduces the TF. The maximum TF that could be calculate by this method was 1.2. The point on Figure 8 is plotted at the wall and roof thickness of TRANSITE for House A and indicates the transmission calculated by Monte Carlo for House A. The transmission is less than the spherical model, as expected, because the openings and rectangular geometry reduce the total capture source and transport to the detector. This indicates that it would be impossible to achieve TF on the order of 1.4 with the cross sections used in our calculations, because this spherical model maximized the contribution from neutron-induced gamma rays. Since excellent agreement is obtained for the neutrons and ^{60}Co gamma rays, the discrepancy does not lie in our geometry model of the house or the radiation transport procedure.

It is possible that a strong secondary gamma-ray producer is present in the TRANSITE, so that either the cross sections used in the computations for the given composition are in error, that the large producer is among the elements detected but not incorporated in the calculations, or that the large producer was not detected in the analysis of the TRANSITE samples. The elements not incorporated in the cross-section set for the calculations account for 0.04% of the total mass (see Table 2). A bounding analysis of gamma-ray production

Table 5. Comparison of Transmission Data for House A at the BREN and HARDTACK Tests

Location	Neutron Transmission Factor			Gamma-ray Transmission Factor		
	BREN		HARDTACK Measured	BREN		HARDTACK Measured
	Measured	Calculated		Measured	Calculated	
E 5 ft	0.46	0.44	0.41	1.44	1.02	1.08
H 3 ft	0.41	0.43	0.35	1.32	0.98	0.98

for these elements indicates they could not account for the 60% increase in the neutron to gamma-ray TF (see Table 4) required to produce agreement. By the same token, it is possible but not probable that the cause is due to cross-section errors or missing elements in the analysis.

Additional evidence indicates that the gamma-ray TF measurements may be in error. Similar house TF measurements made during the nuclear weapon explosions of Operation HARDTACK were examined.[20] During HARDTACK, the House A TRANSITE houses were exposed to low yield nuclear weapons with hard neutron output spectra similar to BREN and at source elevation angles similar to the BREN experiments. A comparison of results reported from the HARDTACK measurements with the BREN data is shown in Table 5. Our calculations are also presented for the BREN experiments. Note in Table 5 that the neutron TF are reasonably consistent with one another, but that our calculations of the gamma-ray TF for BREN agree better with the HARDTACK data than the measured data at BREN. The gamma-ray measurements at HARDTACK were made with a chemical dosimeter system. In conjunction with the same anomalous high gamma-ray measurements in the FIA kerma,[22] it was concluded at this time that the measured gamma-ray reported doses at BREN are probably in error due to either a calibration error or to neutron contamination of the Geiger detectors.

It is instructive to examine the in-house kerma as a function of the point of incidence of the external radiation field. The results can be invaluable for devising generalized TF models for application to Japanese A-bomb dosimetry. Tables 6 and 7 present the fraction of the kerma in the building according to the incidence on the large front opening, the front and rear roof. "Front" and "rear" refer to directions facing toward and away from the source, respectively, and do not correspond in this case to what is normally called the "front" and "rear" of the house. For example, in Table 6, 0.2 × (FIA kerma) was detected at the 3 ft B location from radiation incident on the house through the front opening. The "residual" column tabulates kerma from incidence on the remaining house features. Data in Table 6 for ^{60}Co indicate that for these detector locations the radiation through the front opening and the front roof dominate the detected kerma. As one moves farther back into the house, the reduction in TF is caused by the reduction in the kerma from radiation incident on these house features. Similar conclusions can be made from the data exhibited in Table 7 for the neutron source. The higher fraction of dose from the residual components indicate the neutron field is less forward peaked, as expected.

Table 6. Fraction of Total Exposure Kerma Relative to Free-in-air Kerma from Radiation Incident on House Components. For House A Placed at 750 Yards Ground Range and ^{60}Co Source at Height of 1125 Feet

Detector		House Component				Total Transmission Factor
Location	Height	Front Opening	Front Roof	Rear Roof	Residual	
B	3ft	0.20	0.36	0.003	0.067	0.63
E	3	0.18	0.30	0.01	0.06	0.55
E	5	0.10	0.22	0.01	0.08	0.41
H	3	0.11	0.22	0.03	0.08	0.44

Table 7. Fraction of Total Exposure Kerma Relative to Free-in-air Neutron Kerma Radiation Incident on House Components. For House A Placed at 750 Yards Ground Range and ^{60}Co Source at Height of 1125 Feet

Detector		House Component				Total Transmission Factor
Location	Height	Front Opening	Front Roof	Rear Roof	Residual	
E	3ft	0.15	0.19	0.03	0.11	0.48
E	5	0.09	0.20	0.03	0.12	0.44
G	5	0.02	0.07	0.08	0.27[a]	0.44
H	3	0.08	0.14	0.08	0.13	0.43
H	5	0.05	0.13	0.08	0.12	0.38

[a]Of this residual 0.10 is due to radiation incident on an adjacent window

Calculations for House B. A model for a two-story Japanese house used at BREN was called House B. Our rendition of House B used in the transport calculations is shown in Figures 9 and 10. TF were calculated for the HPRR neutron and the ^{60}Co gamma-ray sources at detector locations indicated in Figure 10. The comparison of our calculations with experimental data is given in Table 8. The source ground range and height were identical to those for House A. The source location column in Table 8 refers to the direction toward the source referenced to the directions indicated in Figure 10. These comparisons show excellent agreement between calculation and measurement. The geometry of House B is considerably more complex than House A, and the good agreement with some "difficult" detector locations indicates the ability of the transport calculations to treat adequately the effects of partitions, windows, and multiple floors.

Calculations for Multiple House Arrangements. A high building density existed in typical residential neighborhoods of Hiroshima and Nagasaki ATB. In these built-up areas with houses close to each other, the shielding effect of adjacent houses is important. To examine the multiple house shielding, the BREN experimenters placed the houses close together in a variety of arrangements and orientations with respect to the sources of radiation.

Two simple house arrangements were calculated in our validation: one for the ^{60}Co source and one for the HPRR. The BREN experimenters did not use an identical arrangement and orientation of House A and House B for both ^{60}Co and the HPRR. The two-house

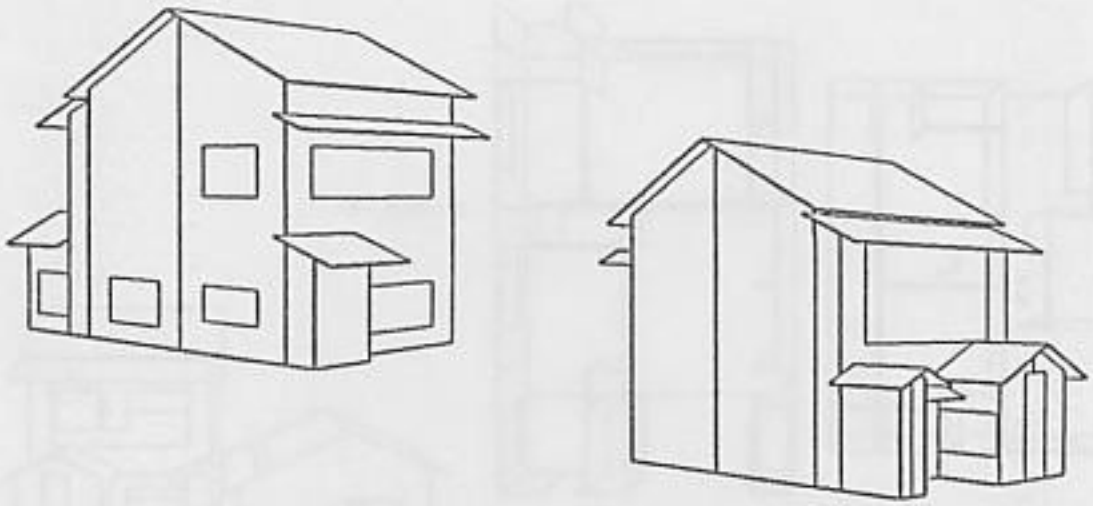

Figure 9. Geometry model of house Type B

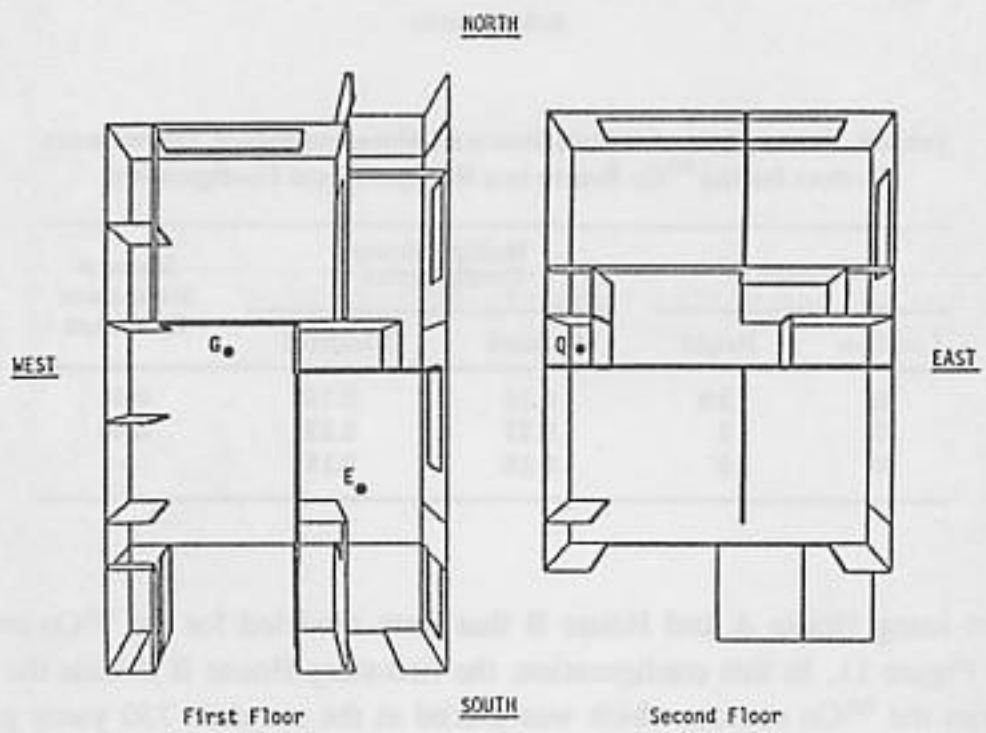

Figure 10. Interior of House B showing calculated location of detector

Table 8. Comparison of Calculations with Measurements of Transmission Factors for House B

Source Location	Detector		^{60}Co Gamma-rays		HPRR Neutrons	
	Location	Height	Measured	Calculated	Measured	Calculated
South	G	5 ft	0.58	0.55	0.38	0.40
East	G	5	0.29	0.26	-	-
South	E	3	-	-	0.50	0.43
South	Q	5	-	-	0.44	0.40

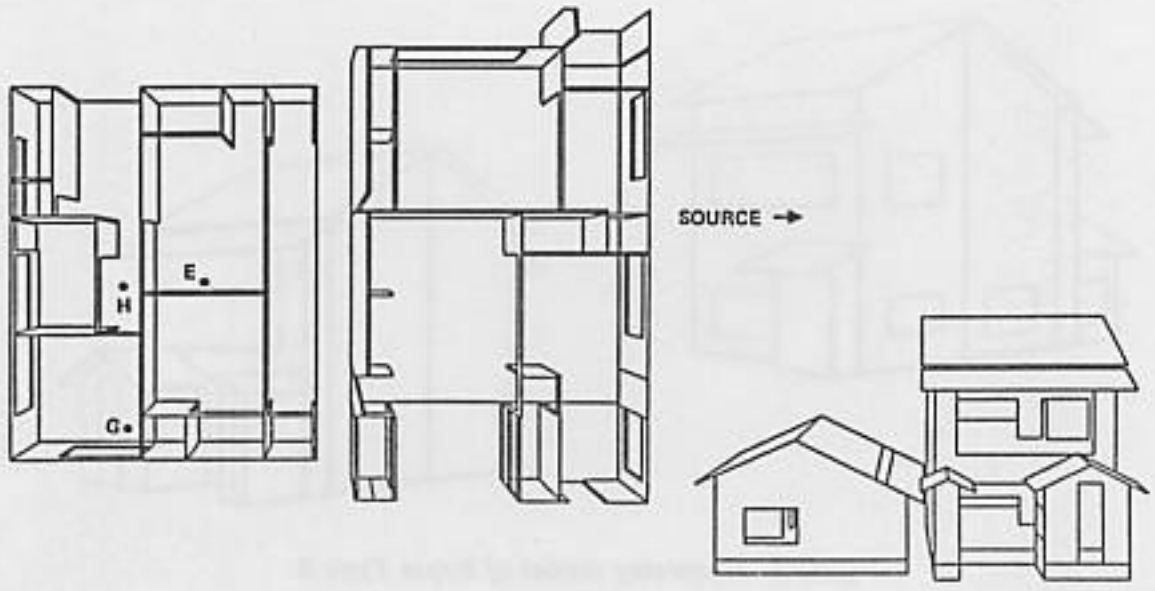

Figure 11. Multiple house configuration for ^{60}Co transmission factor calculations

Table 9. Comparison of Calculations with Measurements of Transmission Factors for the ^{60}Co Source in a Multiple House Configuration

Detector		Multiple House Configuration		House A Stand-alone Calculated
Location	Height	Measured	Calculated	
E	3ft	0.16	0.18	0.48
G	3	0.27	0.22	0.44
H	3	0.16	0.18	-

configuration using House A and House B that were modeled for the ^{60}Co measurements is shown in Figure 11. In this configuration, the two-story House B shields the single-story House A from the ^{60}Co source, which was placed at the standard 750 yards ground range and 1125 feet high.

Calculations were compared with experiment at three detector locations in House A. The results are given in Table 9. The agreement is very good. Also shown in Table 9 for comparison are our calculations of the TF for House A without the intervening House B (reproduced from Table 3). This data indicates that House B in this configuration provides, roughly, the same amount of shielding as House A, which contained the detector.

The configuration used for the HPRR source is shown in Figure 12. Note that the arrangement of House A with respect to House B and the orientation of the source are different from the ^{60}Co source configuration. Three locations in House A and one location in House B were calculated, and the results are provided in Table 10. The agreement between calculation and experiment is excellent. A surprising result was the increase in transmission at location E with the addition of House B on the side. Evidently, House B acts as a scatter source of neutrons that increases the kerma in House A at location E. The situation is reversed

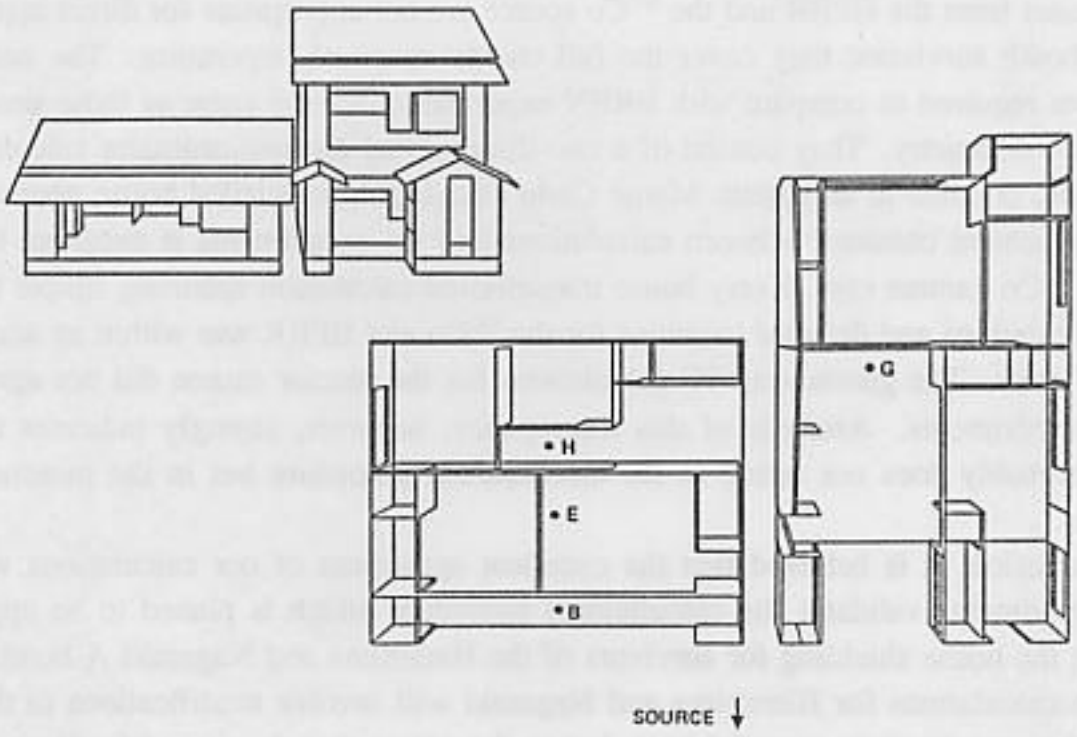

Figure 12. Multiple house configuration for HPRR transmission factor calculations

Table 10. Comparison of Calculations and Measurements of Neutron Transmission Factors for the HPRR Source in a Multiple House Configuration

Detector		Multiple House Configuration		House A Stand-alone Calculated
Location	Height	Measured	Calculated	
B	3 ft	0.65	0.60	-
E	3	0.60	0.60	0.48
H	5	0.32	0.30	0.38
G[a]	3	0.32	0.35	-

[a]Detector first floor of House B

for the 5 ft H location. Note, however, that for location H, House B blocks a large opening on the side and the mid-room partition shields scattered neutrons from the front portions of the side wall of House B. These results are not obvious a priori, but the agreement between experiment and calculation for both the single and multiple configuration confirms them.

Summary and Conclusions

The BREN house transmission experiments provide an excellent set of measurements to validate the calculational procedures that will be used to derive house shielding estimates for the revised dosimetry of the survivors of the Hiroshima and Nagasaki A-bombs. The BREN experiments were performed in realistic full scale models of Japanese residences. Although the radiation spectra and relative intensities of neutrons and gamma rays incident

on the houses from the HPRR and the ^{60}Co source are not appropriate for direct application to the A-bomb survivors, they cover the full energy range of importance. The codes and calculations required to compare with BREN experiments are the same as those needed for the A-bomb dosimetry. They consist of a two-dimensional discrete-ordinates calculation of the free field coupled to an adjoint Monte Carlo calculation in detailed house geometry.

The agreement obtained between calculations and the experiments is excellent for neutrons and ^{60}Co gamma rays. Every house transmission calculation spanning simple to complex configurations and detector locations for the ^{60}Co and HPRR was within an acceptable margin of error. The gamma-ray TF calculations for the reactor source did not agree well with the experiments. Analysis of this discrepancy, however, strongly indicates that the problem probably does not reside in the calculational procedure but in the measurements themselves.

In conclusion, it is believed that the excellent agreement of our calculations with the BREN experiments validates the calculational procedure which is planed to be applied to estimating the house shielding for survivors of the Hiroshima and Nagasaki A-bombs. Certainly, the calculations for Hiroshima and Nagasaki will involve modifications to the code used for the computations reported here, but to the extent that these modifications involve increased calculational complexity to treat more realistic materials and configurations, the benchmark established by these comparisons with the BREN experiments provides a valuable point of departure.

References

1. U.S. Department of Energy, 1982. *Reevaluations of Dosimetric Factors, Hiroshima and Nagasaki*, V. P. Bond and J. W. Thiessen, Eds. Washington: Department of Energy report CONF-810928.
2. Radiation Effects Research Foundation, 1983. *U.S.-Japan Joint Workshop for Reassessment of Atomic Bomb Radiation Dosimetry in Hiroshima and Nagasaki*. Hiroshima: Radiation Effects Research Foundation.
3. Radiation Effects Research Foundation, 1984. *Second U.S.-Japan Joint Workshop for Reassessment of Atomic Bomb Radiation Dosimetry in Hiroshima and Nagasaki*. Hiroshima: Radiation Effects Research Foundation.
4. Auxier, J. A., 1977. *Ichiban: Radiation Dosimetry for the Survivors of the Bombings of Hiroshima and Nagasaki*. Washington: Department of Energy, report TID-27080.
5. Cheka, J. S., Sanders, F. W., Jones, T. D., and Shinpaugh, W. H., 1965. *Distribution of Weapons Radiation in Japanese Residential Structures*. Washington: Department of Energy, report CEX-62.11.
6. Woolson, W. A., Marcum, J., Scott, W. H., and Staggs, V. E., 1982. Building transmission factors. *In Reevaluations of Dosimetric Factors, Hiroshima and Nagasaki*, V. P. Bond and J. W. Thiessen, Eds., pp. 179-200. Washington: Department of Energy report CONF- 810928.
7. Beebe, G. W. and Usagawa, M., 1968. *The Major ABCC Samples*. Hiroshima: Radiation Effects Research Foundation, ABCC report TR-12-68.
8. Kerr, G. D., 1979. Organ dose estimates for the Japanese atomic bomb survivors. Health Physics 37:487-508.
9. Atomic Bomb Casualty Commission, 1964. Calculation method of dose received by those exposed within Japanese-type houses, memorandum for record, Field Operations Section. Hiroshima: Radiation Effects Research Foundation.

10. Marcum, J., 1981. *House Attenuation Factors for Radiation at Hiroshima and Nagasaki.* Marina del Rey, CA: R and D Associates, unpublished report.

11. Hoffman, T. J., 1972. The adjoint difference method and its application to deep-penetration radiation transport. Nucl. Sci. Eng. 48:179.

12. Rhoades, W. A., 1974. *Development of a Code System for Determining Radiation Protection of Armored Vehicles (The VCS Code).* Oak Ridge, TN: Oak Ridge National Laboratory, report ORNL-TM-4664.

13. Gritzner, M. L., 1975. *A User's Manual for the Two-Dimensional Discrete Ordinates Code, DOTSAI.* La Jolla, CA: Science Applications International Corporation, report SAI-75-747-HU.

14. Straker, E. A., Scott, W. H., and Bryn, N. R., 1972. *The MORSE Code with Combinatorial Geometry. Washington:* Defense Nuclear Agency, report DNA-2860T.

15. Scott, W. H. and Staggs, V. E., 1981. *Adjoint Energy Biasing and Thermal Neutron Diffusion in the MORSE and VCS Codes.* La Jolla, CA: Science Applications International Corporation, report SAI-133-81-384-LJ.

16. Auxier, J. A., Sanders, F. W., Haywood, F. F., Thorngate, J. H., and Cheka, J. S., 1962. *Technical Concept - Operation BREN.* Washington: Department of Energy, report CEX-62.01.

17. Auxier, J. A., 1965. The Health Physics Research Reactor. Health Physics 11:89-93.

18. Wagner, E. B. and Hurst, G. S., 1961. A Geiger-Mueller gamma-ray dosimeter with low neutron sensitivity. Health Physics 5:20-26.

19. Wagner, E. B. and Hurst, G. S., 1958. Advances in the standard proportional counter method of fast neutron dosimetry. Rev. Sci. Instr. 29:153.

20. Auxier, J. A., Cheka, J. S., and Sanders, F. W., 1960. *Attenuation of Weapons Radiation: Application to Japanese Houses, Operation Hardtack.* Oak Ridge, TN: Oak Ridge National Laboratory, report WT-1725.

21. Oak Ridge National Laboratory, 1959. *Health Physics Division Annual Progress Report,* pp. 121-124. Oak Ridge, TN: Oak Ridge National Laboratory, report ORNL-2806.

22. Dolatshahi, F. and Kaul, D. C., 1984. *Calculations of Neutron and Gamma-Ray Transport in Air-Over-Ground Geometry - Comparisons of BREN and APR Experiments.* Schaumberg, IL: Science Applications International Corporation, unpublished report.

23. Loewe, W. E., Turin, W. A., Pollock, C. W., Springer, A. C., and Richardson, B. L., 1983. Validated deep-penetration, air-over-ground, neutron/gamma ray transport. Nucl. Sci. Eng. 85:87-115.

24. Kerr, G. D., 1983. Private communication (from intra-laboratory correspondence from J. F. Emery to G. D. Kerr, Jan 19, 1983).

25. Roussin, R. W., 1977. *PVC -36 Group, P_5 , Photon Interaction Cross 5 Sections for 38 Materials in ANISN Format.* Oak Ridge, TN: Oak Ridge National Laboratory, reportk DLC-48.

26. Bartine, D. E., Knight, J. R., Pace, J. V., III, and Roussin, R., 1977. *Production and Testing of the DNA Few-Group Coupled Neutron-Gamma Cross-Section Library.* Oak Ridge, TN: Oak Ridge National Laboratory, report ORNL/TM-4840.

27. Shreve, D. C., 1983. Private communication.

28. Engle, W. W., Jr., 1967. *A User's Manual for ANISN.* Oak Ridge, TN: Oak Ridge National Laboratory, report K-1693.